

ARMY RESEARCH LABORATORY



**Towards Mechanochemistry of Fracture and Cohesion:
Mechanics of a Catenary Process Zone**

by Michael A. Grinfeld and Steven B. Segletes

ARL-TR-5310

September 2010

NOTICES

Disclaimers

The findings in this report are not to be construed as an official Department of the Army position unless so designated by other authorized documents.

Citation of manufacturer's or trade names does not constitute an official endorsement or approval of the use thereof.

Destroy this report when it is no longer needed. Do not return it to the originator.

Army Research Laboratory

Aberdeen Proving Ground, MD 21005-5066

ARL-TR-5310

September 2010

Towards Mechanochemistry of Fracture and Cohesion: Mechanics of a Catenary Process Zone

Michael A. Grinfeld and Steven B. Segletes
Weapons and Materials Research Directorate, ARL

REPORT DOCUMENTATION PAGE			Form Approved OMB No. 0704-0188		
Public reporting burden for this collection of information is estimated to average 1 hour per response, including the time for reviewing instructions, searching existing data sources, gathering and maintaining the data needed, and completing and reviewing the collection information. Send comments regarding this burden estimate or any other aspect of this collection of information, including suggestions for reducing the burden, to Department of Defense, Washington Headquarters Services, Directorate for Information Operations and Reports (0704-0188), 1215 Jefferson Davis Highway, Suite 1204, Arlington, VA 22202-4302. Respondents should be aware that notwithstanding any other provision of law, no person shall be subject to any penalty for failing to comply with a collection of information if it does not display a currently valid OMB control number. PLEASE DO NOT RETURN YOUR FORM TO THE ABOVE ADDRESS.					
1. REPORT DATE (DD-MM-YYYY) September 2010		2. REPORT TYPE Final		3. DATES COVERED (From - To) October 2009-November 2009	
4. TITLE AND SUBTITLE Towards Mechanochemistry of Fracture and Cohesion: Mechanics of a Catenary Process Zone			5a. CONTRACT NUMBER		
			5b. GRANT NUMBER		
			5c. PROGRAM ELEMENT NUMBER		
6. AUTHOR(S) Michael A. Grinfeld Steven B. Segletes			5d. PROJECT NUMBER AH80		
			5e. TASK NUMBER		
			5f. WORK UNIT NUMBER		
7. PERFORMING ORGANIZATION NAME(S) AND ADDRESS(ES) U.S. Army Research Laboratory ATTN: RDRL-WMP-C Aberdeen Proving Ground, MD 21005-5066			8. PERFORMING ORGANIZATION REPORT NUMBER ARL-TR-5310		
9. SPONSORING/MONITORING AGENCY NAME(S) AND ADDRESS(ES)			10. SPONSOR/MONITOR'S ACRONYM(S)		
			11. SPONSOR/MONITOR'S REPORT NUMBER(S)		
12. DISTRIBUTION/AVAILABILITY STATEMENT Approved for public release; distribution is unlimited.					
13. SUPPLEMENTARY NOTES This document is part of a series of reports.					
14. ABSTRACT In this report, a one-dimensional model of cohesion and fracture is examined for flexible substrates (such as tape or hooked fasteners). The process zone is modeled to contain cohesive springs that apply a constant force per unit cracklength, up to the point where a critical displacement of decohesion is reached. This particular model resulted in a crack that takes on a catenary geometry in the process zone. Interestingly, the process zone was found to have a deterministic finite size. More importantly, however, the force relations that resulted from the model were found to match exactly those of a simple cohesion model formulated using the variational method with a macroscopic formulation.					
15. SUBJECT TERMS process zone, fracture, film, bond, catenary, adhesion					
16. SECURITY CLASSIFICATION OF:			17. LIMITATION OF ABSTRACT UU	18. NUMBER OF PAGES 36	19a. NAME OF RESPONSIBLE PERSON Steven B. Segletes
a. REPORT Unclassified	b. ABSTRACT Unclassified	c. THIS PAGE Unclassified			19b. TELEPHONE NUMBER (Include area code) 410-278-6010

Contents

List of Figures	v
1. Introduction	1
2. The Idealized Problem	1
3. Formulating the Boundary Conditions and Governing Equation	4
3.1 The Domain $x < S_f$: The Detached Zone	4
3.2 The Domain $x > S_i$: The Bonded Zone	4
3.3 The Domain $S_f \leq x \leq S_i$: The Process Zone.....	5
3.3.1 The Boundary Conditions	5
3.3.2 The Governing Equation.....	5
4. The Solution	7
4.1 The Catenary Solution Applied to the Domain $S_f \leq x \leq S_i$	7
4.2 Process-Zone Cracklength.....	9
4.3 Bonding Force F_0	11
4.4 The Relation of Applied Tension T_0 to Load Angle θ_0	13
4.5 T_∞ and an Interesting Relationship	14
4.6 Total Field Energy of the Bond and the Work of Deformation	16
4.7 Axial Cable Displacement with Changes in θ_0	19
4.8 The Question of Asymptotes	20

5. Conclusions	21
6. References	22
Appendix. The Catenary Solution	23
Distribution List	25

List of Figures

Figure 1. The system under consideration, characterized by two bonded cables being debonded under an applied load.	2
Figure 2. The $+y$ configuration of an idealized experiment [the $-y$ configuration (not shown) is symmetric about the x -axis], in which two inextensible but flexural cables that have been bonded and attached to the laboratory at point P are “unzipped” by applying an ever-increasing tension T_0 through points H and $-H$ (not shown).	3
Figure 3. Force balance on an element of bonded cable in the idealized process zone.	6
Figure 4. The process-zone shape (aspect ratio 1:1), with the load angle θ_0 as a parameter. ...	10
Figure 5. The process-zone shape, where the x -coordinate has been normalized by Δ , with the load angle θ_0 as a parameter.	10
Figure 6. Normalized x -component (Δ/u_0) and pathwise (s/u_0) size of process zone vs. angle of applied load θ_0 , expressed on a (a) linear and (b) semi-logarithmic scale.	12
Figure 7. The averaged cable angle within the process zone vs. the load angle θ_0	13
Figure 8. Normalized applied force T_0/σ and bonding force F_0/σ vs. angle of applied load θ_0 , expressed on a (a) linear and (b) semi-logarithmic scale.	15
Figure 9. Field energy (E/ϵ_0) in process-zone bond vs. load angle θ_0 (energy $\sigma s/2$ normalized by ϵ_0 given for reference).	17
Figure 10. Schematic showing the origin of the field energy, in terms of external work applied.	18
Figure 11. Schematic showing lengths associated with cable displacement.	20

INTENTIONALLY LEFT BLANK.

1. Introduction

The problem of bonding two surfaces is important in many aspects of Army technology. The need for bonding may arise when two dissimilar materials require mutual attachment, or when geometric complexity and/or cost preclude the manufacture of an item as a single piece. Bonding requirements may call for a permanent adhesive attachment or, alternately, they may require the ability to debond the items on demand, as in the case of tape or velcro.¹ In some cases, the substrate materials being bonded may be stiff, relative to the bonding material, while in other cases, the substrate materials may be wholly flexible (*e.g.*, tape, velcro). This report focuses on bonds involving flexible substrates.

A successful program in adhesive design requires a knowledge not only of how the intact bond successfully performs, but also of how and when the bond will fail. This report is one in a series of reports (1, 2) in which we examine the nature of bonding between two surfaces, and the energy interchange involved with the creation of new free surfaces (*i.e.*, fracture). In an effort to reduce the problem to its essentials, we attempt to formulate scenarios that are maximally simplified. In this way, the problem can be more fully understood without being lost in mathematical complexity. In this report, a notional experiment is described and analyzed, involving the progressive fracture of a one-dimensional (1-D) idealized bond under controlled loading conditions.

2. The Idealized Problem

In figure 1, we display the closed system that we intend to address in this report. It consists of two cables that have been bonded together, which are being separated in a controlled manner. The word “cable” is used here to convey one-dimensionality, though other arrangements that physically approximate one-dimensionality would apply, such as velcro straps or adhesive tape. The goal of such a notional experiment is to study the manner and degree to which a given load mg will bring about the fracture of the bond, altering the load angle θ_0 .

¹Velcro is a hook-and-loop fastener system, which is a registered trademark of Velcro Industries B.V. In this report, we use the lowercase term “velcro” to refer to generic hook-and-loop fasteners in the style of Velcro.

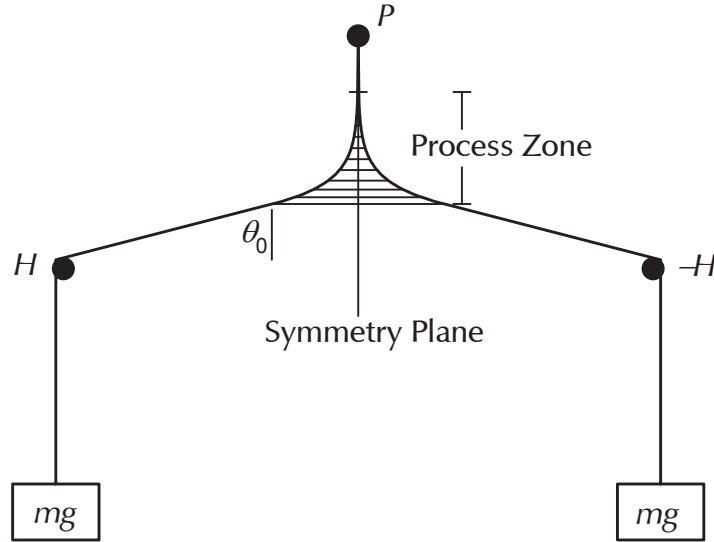


Figure 1. The system under consideration, characterized by two bonded cables being debonded under an applied load.

In figure 1, point P is a rigid attachment point for the bonded cable system. Points H and $-H$ are rigid, frictionless pins, over which the debonded cables respectively pass. The load applied to the cables, brought about by mass m under the influence of gravity g , can and will be, hereafter, characterized by a magnitude of force equal to T_0 .

For the analysis, we focus on a subset of figure 1, as shown in figure 2. In addition to the zoom, figure 2 has been rotated, for convenience, 90° clockwise relative to figure 1. Here, one half of a symmetric system is depicted (*i.e.*, one of the cables), because of planar symmetry across the x -axis. The idealized cables are assumed to be massless, linearly inextensible, yet fully flexible (*i.e.*, incapable of supporting a bending moment). It is important to remember when considering figure 2 that the cable is not attached to point H , but merely directs the applied load T_0 through point H .

The artifice of planar symmetry was introduced to this problem merely to ensure that we were describing a physical system in which the deforming bonds applied force purely in the y -direction. Mathematically, and with no loss of generality, we may solve the half-problem actually shown in figure 2 by considering the cable to lie upon a rigid substrate, under the influence of a perpendicular force-field of specified characteristics. Note, therefore, the descriptive similarity to the thermomechanical problem described in reference 1.

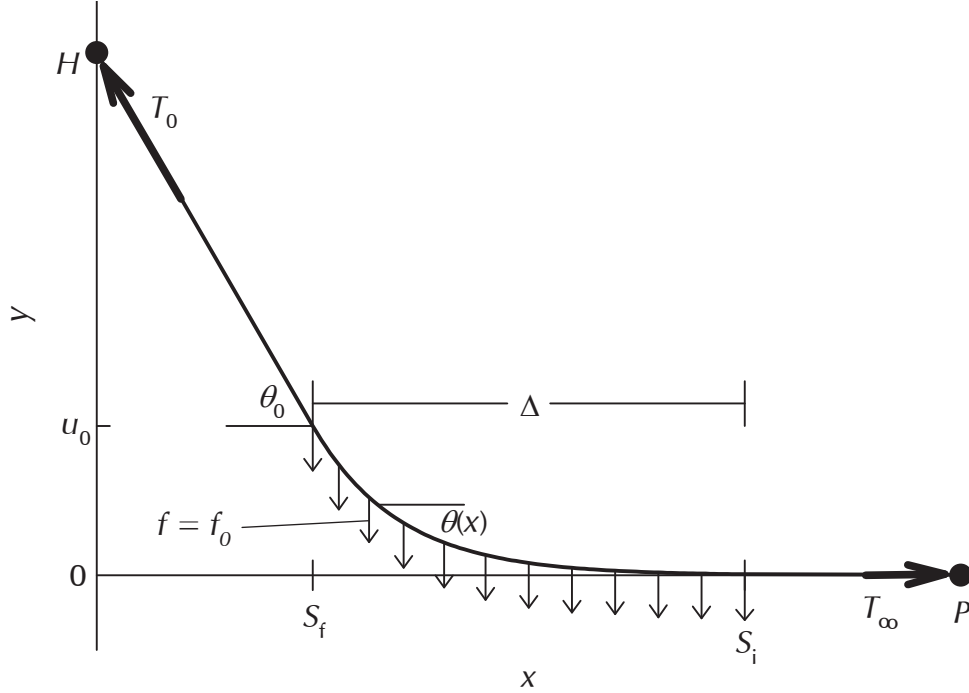


Figure 2. The $+y$ configuration of an idealized experiment [the $-y$ configuration (not shown) is symmetric about the x -axis], in which two inextensible but flexural cables that have been bonded and attached to the laboratory at point P are “unzipped” by applying an ever-increasing tension T_0 through points H and $-H$ (not shown).

In this analysis, we assume the bond provides a fixed resistive force (f_0) per unit length of cable up to the point at which the bond breaks, characterized as when the y -displacement exceeds the critical value for fracture, u_0 . Such process-zone mechanics could be representative of several types of bonding models, for example, a rigid-plastic bond, an electric field, or even a gravitational field. Nonetheless, for a bond resulting from a continuum adhesive, the model is highly simplified, in that transverse (*e.g.*, Poisson) influences on the stress state are ignored.

For points $x < S_f$, the cable is either initially unbonded or has become debonded and remains under load T_0 , applied at an angle θ_0 with respect to the x -axis. The angle θ_0 will change (*i.e.*, decrease) with the progression of the bond fracture, as the load level T_0 is increased.

For cable in the domain $S_f \leq x \leq S_i$, the deforming bond remains intact, but under resistive stress. The restoring force per unit cable-length, given by f_0 , is independent of the y -displacement, u . The tension in the cable, $T(x)$, will not remain fixed in this region, since the stressed bond is applying forces to the cable which are not strictly perpendicular to it. This part

of the problem domain is of x -length Δ , though the pathlength of cable in this domain will always exceed Δ (in fact, it will always be greater than or equal to $\sqrt{\Delta^2 + u_0^2}$).

For the bonded cable, we admit the possibility that beyond a certain domain, $x > S_i$, the y -forces establish a precise balance, such that the cable displacement, u , remains exactly zero. This domain of the cable is still, however, subject to axial tension in the x -direction, given by T_∞ .

The idealized problem, therefore, consists of these three domains: (1) $x < S_f$; (2) $S_f \leq x \leq S_i$; and (3) $x > S_i$. While the problem envisions that the stress states over these domains and indeed the domain limits themselves will change with increasing load, T_0 , the problem we solve here is quasi-static, in which the load T_0 is increased slowly and incrementally, allowing progressive equilibrium states to establish themselves throughout the system. In this manner, we intend to establish a relation that links the magnitude of the applied tension, T_0 , to the resultant level of debonding as characterized by domain boundaries S_f and S_i (alternately expressed as a function of θ_0), in terms of the relevant material parameters (e.g., f_0 and u_0).

3. Formulating the Boundary Conditions and Governing Equation

3.1 The Domain $x < S_f$: The Detached Zone

The domain $x < S_f$ represents that portion of cable that was not bonded to begin with, as well as the additional portion that debonds from the application of force T_0 upon it. The only force acting upon the cable in this domain is the tension applied through point H . Equilibrium considerations dictate that the cable in this domain of the problem remain straight and under constant load, T_0 . There is no requirement that the cable remain forever fixed at point H . Indeed, quite the contrary is required... namely, that the cable be pulled *through* point H as the load T_0 is increased.

3.2 The Domain $x > S_i$: The Bonded Zone

At the far end of the cable, for $x > S_i$ out to point P , the situation is likewise simple to analyze. The cable, in this part of the problem domain, lies upon the x -axis. The force applied where the cable is rigidly attached to point P is given as T_∞ . Force equilibrium dictates, that at all points in this part of the problem domain, the cable tension remain fixed at T_∞ .

Furthermore, by considering the complete length of cable for $x > 0$ as a free body, and knowing that all external forces upon it in the intermediate region ($S_f \leq x \leq S_i$) are perpendicular to the x

axis, a force equilibrium on the cable, applied in the x -direction, leads one to conclude that

$$T_{\infty} = T_0 \cos \theta_0 \quad . \quad (1)$$

3.3 The Domain $S_f \leq x \leq S_i$: The Process Zone

We now proceed to analyze the most important part of the problem—the process zone.

3.3.1 The Boundary Conditions

This part of the problem domain represents the key part of the problem: the deforming bond on its way toward eventual fracture. We may conclude several salient boundary conditions on this domain. Because there are no concentrated forces applied at S_i and/or S_f (only a distributed force along the entire domain), equilibrium applied across the domain boundaries will require a continuity of cable tension, displacement, and slope.

The cable tension (T) changes along the length of cable in this part of the problem domain. However, the tension must be $T = T_0$ at $x = S_f$ and $T = T_{\infty}$ at $x = S_i$, in order to match the adjacent domains. Since the coordinates and slopes of the cable must also match the adjacent domains, this requires that, at $x = S_f$, the y -displacement $u = u_0$ and $u' = -\tan \theta_0$. At the other end of the domain, $x = S_i$, we must satisfy the requirement that $u = 0$, and $u' = 0$.

3.3.2 The Governing Equation

To develop the governing relations for the process zone, we must satisfy the equilibrium requirements for an arbitrary section of cable in that zone, such as that depicted in figure 3.

In the x -direction, the only forces arise from the tension in the cable, and therefore

$$\frac{d}{dx}(T \cos \theta) = 0 \quad . \quad (2)$$

From this, we conclude that $T \cos \theta$ must remain constant, and that constant, from matching the conditions at the end of the domain, is given by

$$T \cos \theta = T_{\infty} = T_0 \cos \theta_0 \quad . \quad (3)$$

In the y -direction, the situation is slightly more complex, in that the independent variable will still be taken as x , even as the forces being summed are y -forces. If F represents the integral along

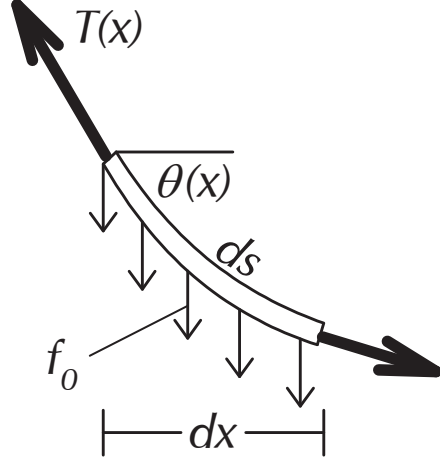


Figure 3. Force balance on an element of bonded cable in the idealized process zone.

the x -direction of the distributed bond force f_0 , then the condition of equilibrium in the y -direction becomes

$$\frac{d}{dx}(T \sin \theta + F) = 0 \quad . \quad (4)$$

One must note, however, that the bonds which produce the distributed force f_0 are distributed along the cable length ds . Therefore, as the angle $\theta(x)$ changes, the density of bonds along dx changes as well. Thus, the quantity dF/dx must be considered as $dF/ds \cdot ds/dx$. The quantity dF/ds is merely the distributed force of the bond, namely f_0 , while ds/dx is obtained from the geometry as $\sec \theta$, alternately expressible as $\sqrt{1 + u'^2}$. Using equation 3, we can reexpress $T \sin \theta$ as $T_\infty \tan \theta$, alternately expressible as $-T_\infty u'$.

Combining all these substitutions into equation 4 yields the following governing relation:

$$u'' - \frac{f_0}{T_\infty} \sqrt{1 + u'^2} = 0 \quad . \quad (5)$$

Equation 5 should be immediately recognized as being associated with the so-called ‘‘catenary’’ solution, which is the curve that governs the geometry of a free-hanging chain or cable under the force of gravity (indeed, the word *catenary* comes from the word *catena*, Latin for chain). Such a connection should not be surprising when one considers that the distributed force of the deforming bonds, f_0 , constant per unit length of cable, is directly analogous to the distributed force of a cable’s weight under the force of gravity.

It may, therefore, be instructive to visualize the solution to this mechanics problem in terms of the analogous gravitational problem, in which a long, heavy chain is laid in a straight line upon a table (the rigid substrate). As a free end of the chain is lifted to a given height above the table (analogous to u_0), the shape in which the hanging chain establishes itself will vary with the level of tension applied (itself being a function of the vertical (lifting) and lateral (stretching) components of that force). The derivation of the catenary solution is provided in the appendix, for the reader's convenience.

4. The Solution

4.1 The Catenary Solution Applied to the Domain $S_f \leq x \leq S_i$

To solve equation 5, let us first make the substitution of convenience that $\alpha = f_0/T_\infty$. Next, we introduce a shifted coordinate system, $\xi = x - S_f$, which allows equation 5 to remain unaltered with respect to ξ , while at the same time redefining the bounds of the domain as $0 \leq \xi \leq \Delta$, where $\Delta = S_i - S_f$.

The general solution to equation 5 is

$$u = Ae^{-\alpha\xi} + Be^{\alpha\xi} + C \quad , \quad (6)$$

where the constants A and B are subject to the constraint

$$2\sqrt{AB} = \frac{1}{\alpha} \quad . \quad (7)$$

Note that equation 7 requires that A and B be of the same sign, so that their product is positive.

The boundary conditions developed in section 3.3.1 require that

$$u(0) = A + B + C = u_0 \quad (8)$$

$$u'(0) = (-A + B)\alpha = -\tan \theta_0 \quad (9)$$

$$u(\Delta) = Ae^{-\alpha\Delta} + Be^{\alpha\Delta} + C = 0 \quad (10)$$

$$u'(\Delta) = -A\alpha e^{-\alpha\Delta} + B\alpha e^{\alpha\Delta} = 0 \quad . \quad (11)$$

Equation 11, upon multiplication by $e^{\alpha\Delta}$ and upon elimination of α by way of equation 7, may be directly solved for Δ as

$$\Delta = \sqrt{AB} \ln(A/B) \quad . \quad (12)$$

From this and equation 7, the following two results follow:

$$\begin{aligned} e^{\alpha\Delta} &= \sqrt{A/B} \\ e^{-\alpha\Delta} &= \sqrt{B/A} \end{aligned} \quad . \quad (13)$$

Substituting these results into equation 10 reveals that

$$C = -2\sqrt{AB} \quad , \quad (14)$$

which also happens to equal the negative reciprocal of α .

Starting with equation 9 and eliminating α with a substitution of equation 7 produces the equation

$$\sqrt{A/B} - \sqrt{B/A} = 2 \tan \theta_0 \quad . \quad (15)$$

This may be solved quadratically, in light of the requirement that A and B be of the same sign, as

$$\sqrt{\frac{A}{B}} = \frac{1 + \sin \theta_0}{\cos \theta_0} \quad . \quad (16)$$

We are now prepared to substitute equation 14 into equation 8, while isolating B , to obtain

$$B \left((A/B) + 1 - 2\sqrt{A/B} \right) = u_0 \quad . \quad (17)$$

This conveniently reduces to

$$B \left(\sqrt{A/B} - 1 \right)^2 = u_0 \quad . \quad (18)$$

The term B may now be directly solved by substituting equation 16 into equation 18 in order to obtain

$$B = \frac{u_0(1 - \sin \theta_0)}{2(1 - \cos \theta_0)} \quad . \quad (19)$$

The quantity A directly follows as

$$A = \frac{u_0(1 + \sin \theta_0)}{2(1 - \cos \theta_0)} \quad . \quad (20)$$

Now that A and B are explicitly known in terms of the boundary conditions, C may also be explicitly calculated by substitution into equation 14:

$$C = \frac{-u_0}{\sec \theta_0 - 1} \quad . \quad (21)$$

The quantity Δ follows from equations 12 as:

$$\Delta = \frac{u_0}{2(\sec \theta_0 - 1)} \ln \left(\frac{1 + \sin \theta_0}{1 - \sin \theta_0} \right) \quad . \quad (22)$$

Thus, our four unknowns, A , B , C , and Δ , have been fully characterized.

These parameters may be employed through equation 6 to trace the shape of the cable within the process zone, where the distributed force f_0 is applied. Figure 4 shows the actual shape of the cable for different load angles θ_0 . For smaller load angles, the curves exit the right side of the graph, because the x -measure of the process-zone size, Δ , exceeds u_0 . Therefore, we provide figure 5, which shows the typical cable geometry for various load angles, except that the x -axis has been normalized by Δ .

Note from figure 5 that the normalized shapes of the curves are all very similar for load angles below 60° . As the load becomes more perpendicularly oriented to the substrate, however, the shape of the cable acquires much more of a knee-like shape to it and the tail becomes longer.

4.2 Process-Zone Cracklength

Now that the shape of the deforming surface of the process zone has been fully defined through the calculation of the parameters A , B , C , and Δ , the process-zone cracklength can be calculated. The process zone is defined by the rectangle $S_f \leq x \leq S_i$ and $0 \leq y \leq u_0$ (refer to figure 2). It spans an x distance of $S_i - S_f$, which we have called Δ and a y distance of u_0 . Equation 22 gives us an explicit measure of the x -component of the zone size. However, Δ is not, strictly speaking, the process-zone cracklength. From figure 3, we note that the length of the crack formed is the integral of ds , not that of dx . Therefore, the full process-zone cracklength s , is obtained as follows:

$$s = \int ds = \int_0^\Delta \sqrt{1 + u'^2} \, d\xi \quad . \quad (23)$$

From directly differentiating and squaring equation 6, it may be verified, in light of equation 7, that

$$\sqrt{1 + u'^2} = \alpha(Ae^{-\alpha\xi} + Be^{\alpha\xi}) \quad . \quad (24)$$

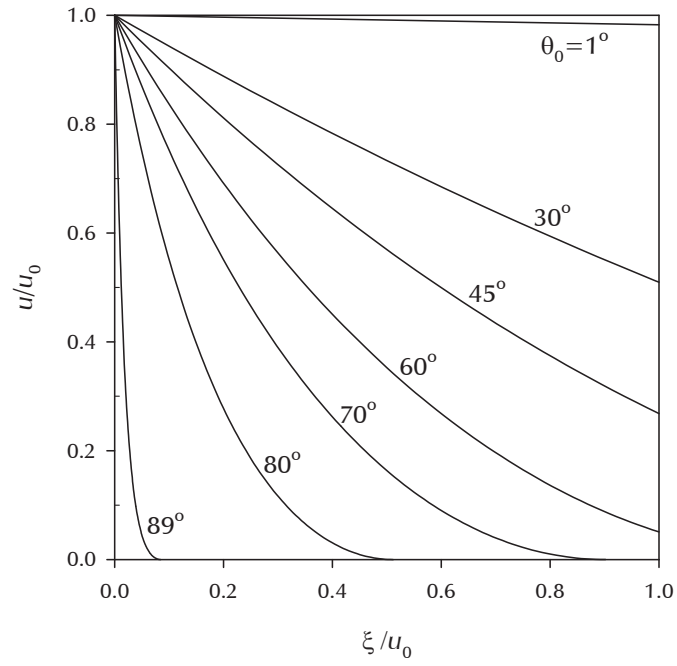


Figure 4. The process-zone shape (aspect ratio 1:1), with the load angle θ_0 as a parameter.

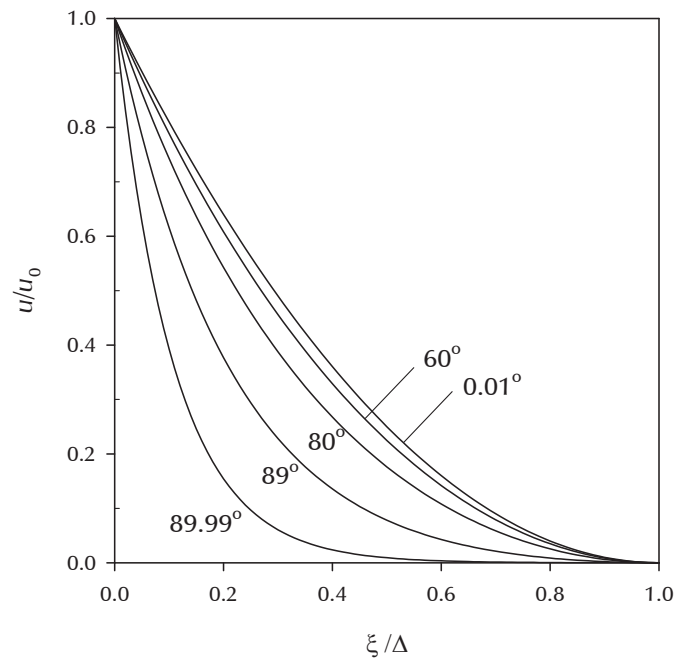


Figure 5. The process-zone shape, where the x -coordinate has been normalized by Δ , with the load angle θ_0 as a parameter.

Integrating equation 24 across the process zone (*i.e.*, from $\xi = 0$ to Δ), in light of equation 13, gives the following value for the cracklength s within the process zone:

$$s = \int_0^{\Delta} \sqrt{1 + u'^2} \, d\xi = A - B \quad . \quad (25)$$

If B and A are explicitly substituted from equations 19 and 20, one obtains the cracklength in the process zone as

$$s = u_0 \cot(\theta_0/2) \quad . \quad (26)$$

A comparison of s to Δ is presented in figure 6. Naturally, $s \geq \Delta$ for all loading angles θ_0 . A specific point of note on figure 6a is the behavior as θ_0 approaches 90° (*i.e.*, applied loading perpendicular to the plane of symmetry). We note that the x -width of the process zone (Δ) approaches zero length. However, the pathlength of cable in the process zone (*i.e.*, the process-zone cracklength s) can never fall below u_0 , because even the limiting case of a process-zone rectangle approaching dimensions $0 \times u_0$, the cable, oriented perpendicular to the plane of symmetry, will retain a cracklength of u_0 .

Knowledge of Δ allows the contents of figure 6 to be presented in a slightly different manner. Namely, $\tan^{-1}(u_0/\Delta)$ represents the average angle of the cable within the process zone. This is shown in figure 7.

4.3 Bonding Force F_0

The bonding force F_0 is also of interest. We define it as the total resistive force in the y -direction applied to the cable in the process zone $S_f \leq x \leq S_i$. We should note that, because of the perpendicularity of F_0 and T_∞ , equilibrium upon the cable dictates that $T_0^2 = F_0^2 + T_\infty^2$. The resistive force comprising F_0 is uniformly distributed along the cable length with a constant magnitude of f_0 per unit cable length. Therefore, calculating the total bonding force is straightforward:

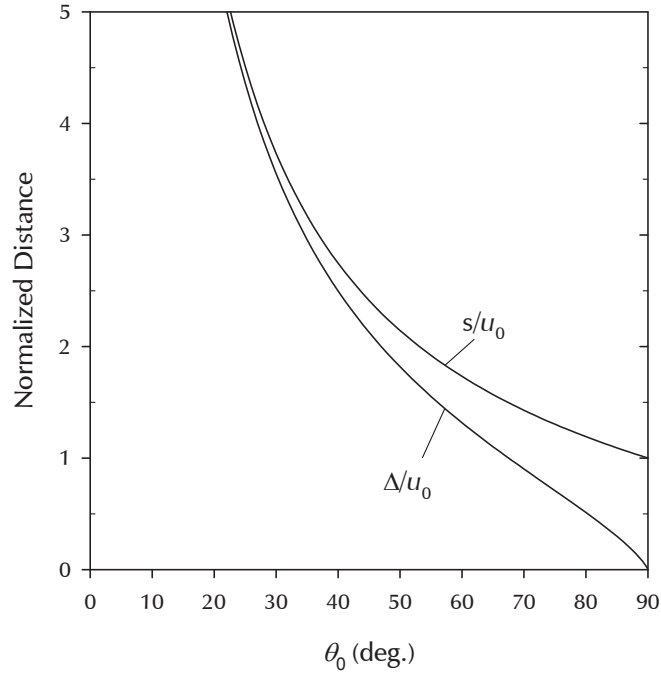
$$F_0 = f_0 s \quad . \quad (27)$$

Substituting from equation 26, and introducing the term grouping

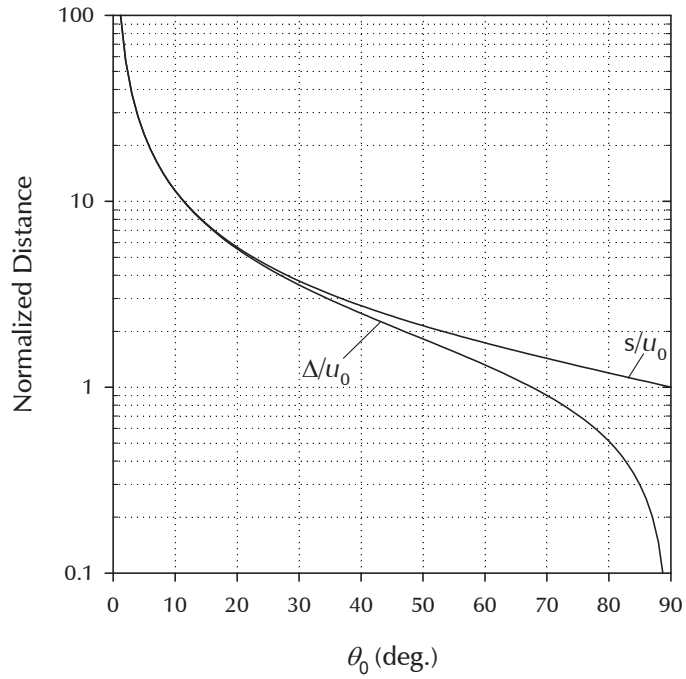
$$\sigma = f_0 u_0 \quad , \quad (28)$$

the total bonding force is obtained as

$$F_0 = \sigma \cot(\theta_0/2) \quad . \quad (29)$$



(a)



(b)

Figure 6. Normalized x -component (Δ/u_0) and pathwise (s/u_0) size of process zone vs. angle of applied load θ_0 , expressed on a (a) linear and (b) semi-logarithmic scale.

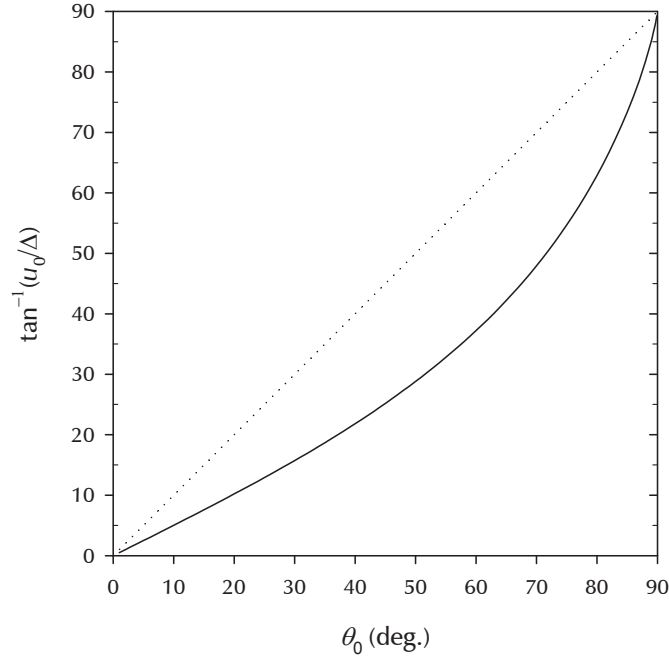


Figure 7. The averaged cable angle within the process zone vs. the load angle θ_0 .

In equation 28, the product of the distributed bonding force per unit cracklength and the critical displacement to bring about full fracture represents the work per unit cracklength required to completely fracture the bond. Thus, σ is a material property that may be termed the specific bond energy (*e.g.*, the bond energy per unit cracklength).

Therefore, equation 29 shows the total bonding force to be directly proportional to the specific bond energy σ and the cotangent of the half-angle of the applied force. In the limiting case of a $\theta_0 = 90^\circ$ applied load, the total bonding force (F_0) exactly equals the specific bond energy σ . This result should not be surprising in light of section 4.2, which showed the minimum size of the process-zone cracklength to be u_0 as the load angle θ_0 approaches 90° . Since the bonding force F_0 is proportional to the process-zone cracklength s and not merely the x -component of cracklength Δ , the bonding force can never fall below the specific bond energy σ , even as Δ approaches zero length.

4.4 The Relation of Applied Tension T_0 to Load Angle θ_0

The bond force F_0 , which is known explicitly, may be used to calculate the ultimately desired quantity, the tension in the cable required to bring about separation angle θ_0 . From geometry, we know that, in order to satisfy y -equilibrium, the y -component of tension must exactly equal the

bonding force F_0 . Thus,

$$T_0 = \frac{F_0}{\sin \theta_0} = \frac{\sigma}{2 \sin^2(\theta_0/2)} \quad (30)$$

Therefore,

$$\sin\left(\frac{\theta_0}{2}\right) = \sqrt{\frac{\sigma}{2T_0}} \quad (31)$$

This is precisely the relation obtained in reference 1 where the analogous problem was solved using variational principles of energy exchange between a hanging mass m and the specific chemical energy σ of the bond, which supports the mass through a cable bonded to a rigid substrate. In that solution, the tension applied to the bond at an angle θ_0 arises from a weight, given by mg . However, in the variational approach, the mechanics of the problem are not even addressed and, thus, it was a bit unexpected (though fully welcomed) to achieve exactly the same result.

4.5 T_∞ and an Interesting Relationship

The quantity T_∞ is the only force quantity left to calculate. It is easily obtained as

$T_\infty = T_0 \cos \theta_0$, which reduces to the following:

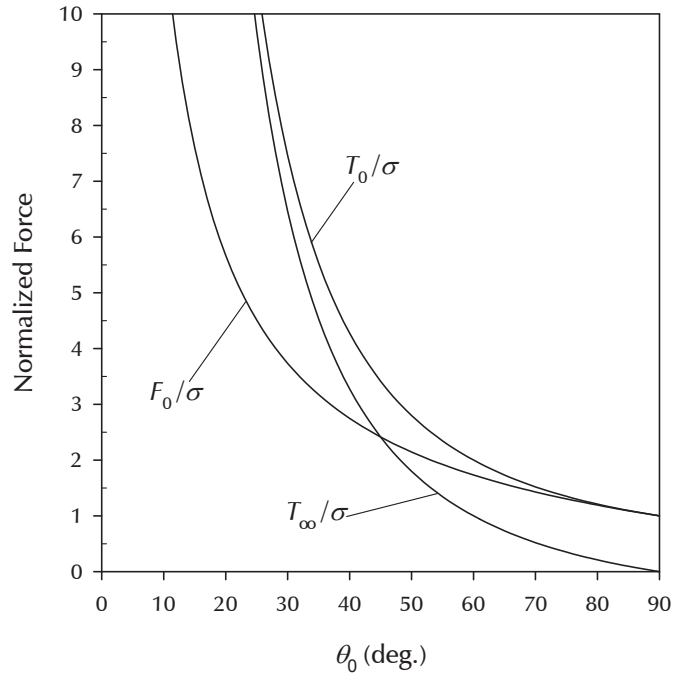
$$T_\infty = \frac{\sigma}{\sec \theta_0 - 1} \quad (32)$$

Figure 8 presents the relation of the applied cable tension T_0 , the total bonding force F_0 , and T_∞ as a function of the applied-load angle θ_0 . Above load angles of 45° , F_0 will exceed T_∞ in magnitude. Below 45° , the reverse is true. In all cases, T_0 exceeds the other forces because it is the hypotenuse associated with the components F_0 and T_∞ .

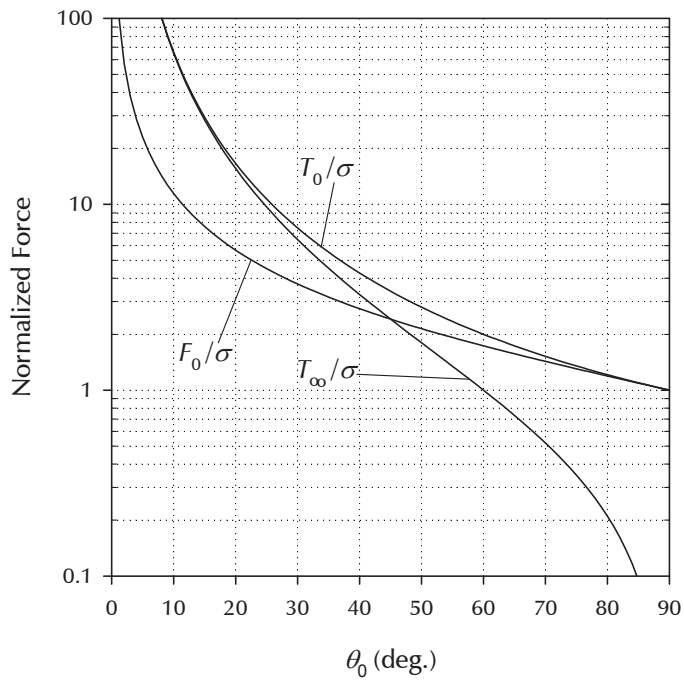
One very interesting relation that may be shown is that

$$T_0 - T_\infty = \sigma \quad (33)$$

regardless of the angle of applied force, θ_0 . That the difference of T_0 and T_∞ should remain invariant may be understood in the following way. Every segment of cable in the process zone is subjected to a distributed y -force of magnitude f_0 . For each segment, there is a component of that distributed force which is directed along the cable length, thereby changing the magnitude of the cable tension. This distributed component directed along the cable is of magnitude $f_0 \sin \theta$, where θ varies from 0 to θ_0 through the process zone. The overall change in the cable tension, therefore, is $\int_0^{\theta_0} f_0 \sin \theta \, ds$. The quantity f_0 , being constant, may be taken out of the integral,



(a)



(b)

Figure 8. Normalized applied force T_0/σ and bonding force F_0/σ vs. angle of applied load θ_0 , expressed on a (a) linear and (b) semi-logarithmic scale.

while the remaining integrand ($\sin \theta ds$) is simply du . The change in cable tension is, therefore, $f_0 \int_0^{u_0} du = f_0 u_0 = \sigma$, which is independent of the particular geometry of the process zone.

Note that the relationships for F_0 , T_0 , and T_∞ are functions of the term grouping σ , rather than functions of f_0 alone or u_0 alone. What this indicates is that, while f_0 and u_0 were introduced as fundamental model parameters, the calculation of equilibrium loads is really not dependent on their individual respective values, but rather only upon the load angle and the specific bond energy, σ . Where u_0 will play a direct role is in the calculation of the field energy within the process zone itself, as will be shown in section 4.6 of this report.

4.6 Total Field Energy of the Bond and the Work of Deformation

In section 4.5, the specific bond energy, σ , was introduced to describe the energy required to create a unit of cracklength (*i.e.*, to grow the crack). We also have the ability to integrate what would traditionally be called the elastic energy of the bond. In the current model, however, the term “elastic” might not be appropriate, because the force-displacement relationship here is a constant, and not linear with displacement in the traditional sense of elasticity. Additionally, the bonding force may be dissipative, as in the case of a plastic or velcro bond. Therefore, rather than call it “elastic” energy, we will refer to it as the total field energy of the bond. It refers to the integration of energy throughout the process zone, arising from the displacement of the cable from the $u = 0$ configuration:

$$E = \int f_0 u ds = f_0 \int_0^\Delta u \sqrt{1 + u'^2} d\xi \quad . \quad (34)$$

In the simplest case, if the cable geometry were linear within the process zone (rather than catenoid), such that the cable extended linearly from the (x, y) point (S_f, u_0) to $(S_i, 0)$, the total field energy of the bond would be $\sigma s/2$.

Except when the load is applied at 90° , the present solution does not have a linearly varying displacement in the process zone. For the special case of 90° loading, the cable approaches in the limit a y -oriented line in the process zone, of cracklength $s = u_0$. Let us define a baseline field energy as $\epsilon_0 = \sigma u_0/2 = f_0 u_0^2/2$. It represents the energy stored (or dissipated) in the process zone of a bond that is subjected to a y -oriented load (*i.e.*, perpendicular to the plane of symmetry) of limiting magnitude $T_0 = F_0 = \sigma$.

For load angles other than $\theta_0 = 90^\circ$, we would expect (because of the displacement field’s concavity) the total field energy to be less than $\sigma s/2$. Let us proceed to obtain it. Equation 34 may be directly integrated through substitution of equations 6 and 24, in light of equation 13.

The result is given by

$$E = f_0 \left[\frac{A-B}{2}(A+B+C) + \frac{A-B}{2}C + \Delta\sqrt{AB} \right] , \quad (35)$$

which may be reduced to

$$E = \frac{1}{2}[\sigma s - T_\infty(s - \Delta)] , \quad (36)$$

consistent with our expectations. This energy relationship is displayed in figure 9, normalized by ϵ_0 .

To understand the physical origin of equation 36, and how the field energy arises from externally applied work, figure 10 is provided. The point O represents the location $x = S_i$, where $\xi = \Delta$. The actual path representing the cable's deformed state is given by the arc \overline{OB} (of length s). If the cable lying along arc \overline{OB} were not subject to the tension T_0 at point B , the cable would instead lie (unstressed) along the line \overline{OA} .

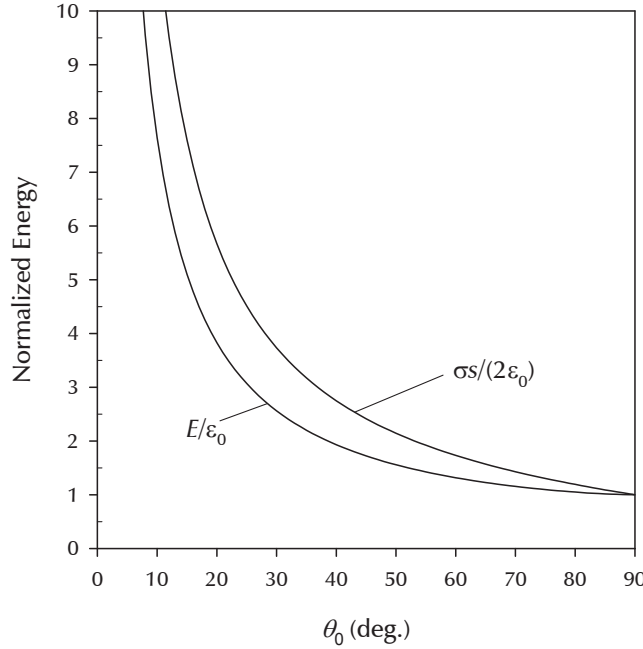


Figure 9. Field energy (E/ϵ_0) in process-zone bond vs. load angle θ_0 (energy $\sigma s/2$ normalized by ϵ_0 given for reference).

We contemplate the application of tension \vec{T} to point A of the unstressed cable, applied at a constant angle of θ_0 (in this case, 60°). The magnitude of the tension would start as 0 when the

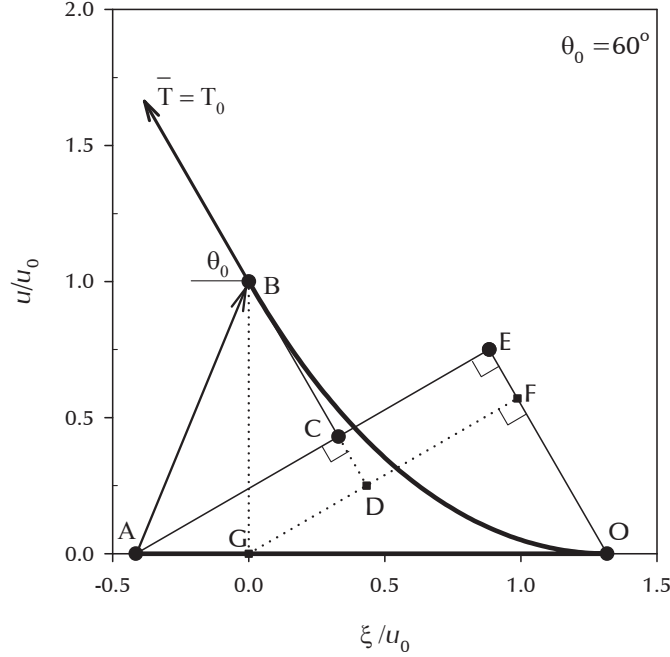


Figure 10. Schematic showing the origin of the field energy, in terms of external work applied.

cable was in the \overline{OA} configuration, increasing to a magnitude of T_0 as the cable reoriented itself to the deformed configuration \overline{OB} . Because the magnitude of tension \vec{T} can be shown directly proportional to the u -displacement of the endpoint, one may assert that the averaged value of tension \vec{T} applied when the point A is deformed to point B is exactly $(0 + T_0)/2 = T_0/2$.

The work W done by this action, as point A moves to B under increasing force \vec{T} , is the integral of the force times the component of displacement in the direction of action, which is $\int \vec{T} \cdot d\vec{AB}$, given more simply as $W = (T_0/2)|\overline{CB}|$. Because \overline{OE} is parallel with \vec{T} , while \overline{AE} and \overline{GF} are perpendicular to it, we can assert that $|\overline{CB}| = |\overline{DB}| - |\overline{OE}| + |\overline{OF}|$. We may further assert, on geometrical grounds, that $\angle FOG = \angle BGD = \theta_0$. Therefore, $|\overline{DB}| = |\overline{GB}| \sin \theta_0 = u_0 \sin \theta_0$. Likewise, $|\overline{OE}| = |\overline{OA}| \cos \theta_0 = s \cos \theta_0$. Finally, we have that $|\overline{OF}| = |\overline{OG}| \cos \theta_0 = \Delta \cos \theta_0$. Substituting all these metrics into the equation representing the work done to deform the cable from the unstressed configuration \overline{OA} to the fully-stressed configuration \overline{OB} gives the following result:

$$W = (T_0/2)[u_0 \sin \theta_0 - (s - \Delta) \cos \theta_0] \quad . \quad (37)$$

Knowing that $T_0 u_0 \sin \theta_0 = F_0 u_0 = \sigma s$ and that $T_0 \cos \theta_0 = T_\infty$ allows equation 37 to be reduced to

$$W = \frac{1}{2}[\sigma s - T_\infty(s - \Delta)] \quad . \quad (38)$$

The identical forms of equations 36 and 38 tell us that the amount of field energy stored in (or dissipated by) the bonds along the cable in the region \overline{OB} exactly equals the external work that would have been required to deform the cable from its stress-free configuration \overline{OA} to its fully loaded configuration \overline{OB} .

4.7 Axial Cable Displacement with Changes in θ_0

Examining the underlying premise of figure 1, it is apparent that, as the cable bond becomes progressively “unzipped,” the weights (each of adjustable mass m) will give up potential energy as they lower in height. In this section, we seek to determine the amount of axial cable displacement (*i.e.*, decrease in height of mass m) that occurs as a function of the load angle θ_0 .

As a reference state, we chose the situation where the initial value of θ_0 is 90° and the initial cable tension exactly equals the associated equilibrium value of $T_0 = \sigma$. As the masses lower and the cables begin to debond, the decrease in cable length between points H and P corresponds exactly to the change in the elevation, Δz , of the masses.

We employ figure 11 to assist in determining cable lengths. Initially, we assume that u_0 (and thus the process zone) is vanishingly small, so that the fractured geometry associated with load angle θ_0 is composed of two segments: the detached cable segment (of length c) and the bonded cable segment (of length $p - a$). Under this assumption, the elevation change of the masses, Δz , when the load angle, θ_0 , deviates from 90° , is given by

$$\Delta z = h + a - c \quad (\text{when } u_0 \ll h) \quad , \quad (39)$$

where $a = h / \tan \theta_0$ and $c = h / \sin \theta_0$.

However, when the size of the process zone is not considered negligible, a further refinement to equation 39 is required to obtain the elevation change of the masses, Δz , when the load angle, θ_0 , deviates from 90° . Employing the relation for s from equation 26 and seeing that $b = u_0 / \sin \theta_0$ and $d = \Delta - u_0 / \tan \theta_0$, we obtain

$$\Delta z = (h + a - c) + (b + d - s) = \frac{h}{\sin \theta_0} (\sin \theta_0 + \cos \theta_0 - 1) + (\Delta - 2u_0 \cot \theta_0) \quad . \quad (40)$$

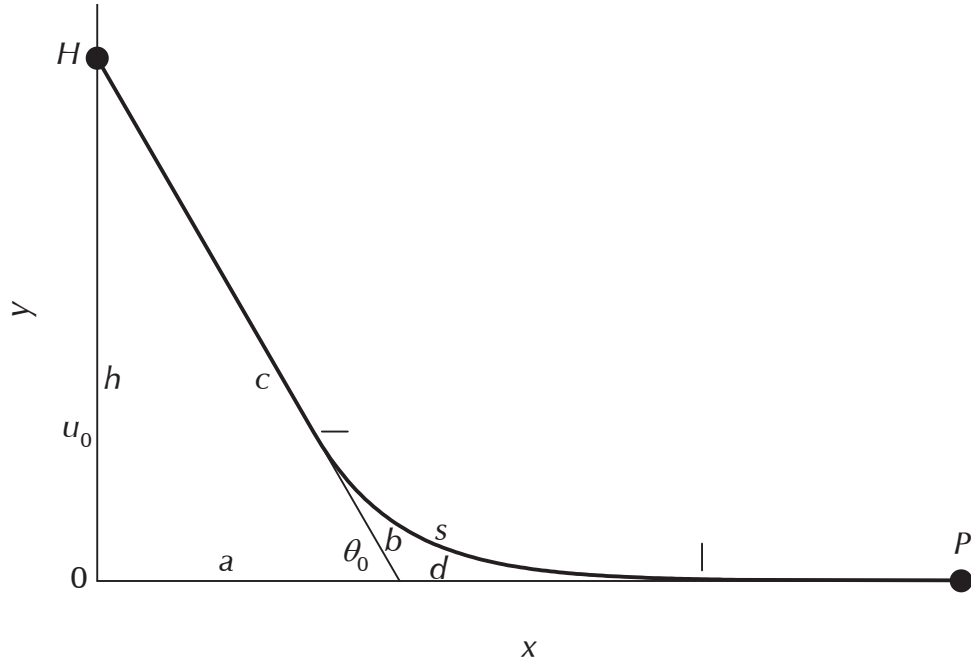


Figure 11. Schematic showing lengths associated with cable displacement.

To repeat, the value of Δz represents the finite change in elevation level of the masses of figure 1 as a function of the load angle θ_0 . An initial value of $\theta_0 = 90^\circ$ is assumed. The first term of equation 40, proportional to h , is the dominant term, arising from the macroscopic geometry of the system. The second term, on the order of u_0 , provides a secondary correction, to account for the catenoid shape of the process zone. Further insight could be pursued, for example, by comparing the displacement, Δz , of the adjustable masses with the debonded cable length, given by $S_f = (h - u_0) / \tan \theta_0$.

4.8 The Question of Asymptotes

One of the questions that arose (in the minds of the authors) during the course of this investigation was whether or not the eventual solution would be asymptotic. That is to say, whether the location of S_i (see figure 2) would approach infinity, even for finite values of T_0 . The present solution shows that, for the current set of governing assumptions, it does not. One mathematical fact regarding asymptotes is that their second derivative approaches zero, since an asymptote's graph approaches a straight line.

Considering equation 5, however, one can see that, as long as the specific bonding force f_0 is nontrivial, u'' must be greater than zero. Thus, the governing equation 5 is incapable of producing an asymptotic result, wherein $u'' = 0$.

This also raises the possibility, however, that were the bonding-force relation something other than a constant, the conclusion regarding the possibility of an asymptotic solution would change as well. For example, instead of a constant specific bond force f_0 , the bond might be characterized by a spring-type $f = ku$ specific bonding force. With such a physical model, the governing relation would become $u'' - (k/T_\infty)u\sqrt{1 + u'^2} = 0$. In this circumstance, it would be mathematically possible to achieve an asymptotic solution, in which u approached zero only as x approached infinity. In such a case, u'' would likewise approach zero, which is the requirement for an asymptote.

5. Conclusions

In this report, a notional experiment was presented involving the progressive debonding of two flexible surfaces (*e.g.*, tape or velcro). An idealized model was developed which, when solved, predicts the shape of the flexible substrate in the process zone where debonding occurs. More importantly, it provides the force and energy relationships that govern the problem as a function of the loading angle, which will provide the means to test the model against future experimental data.

The assumptions contained in the formulation are that (1) the (tape or velcro) substrate is fully flexible; (2) the bonds are one-dimensional in nature, such that there is no lateral (*i.e.*, Poisson) interaction in the process zone; (3) the bonding force in the process zone is independent of separation up to the point of fracture (in the manner of a perfectly-plastic bond); and (4) the bonds are uniformly distributed along the substrate length.

Based on these assumptions to the problem, the process zone was seen to take on the shape of a catenary (*i.e.*, a free-hanging cable under the influence of gravity), for which an analytical solution presents itself. Importantly, the force relations predicted for this model identically matched those developed for the problem using an alternate energy-based approach (1).

6. References

1. Grinfeld, M. A.; Segletes, S. B. *Towards Mechanochemistry of Fracture and Cohesion: General Introduction and the Simplest Model of Velcro*; ARL-TR-XXXX; U.S. Army Research Laboratory: Aberdeen Proving Ground, MD, XXX 2010.
2. Grinfeld, M. A.; Segletes, S. B. *Towards Mechanochemistry of Fracture and Cohesion: Two-Component Spring Models of Velcro Detachment*; In progress; U.S. Army Research Laboratory: Aberdeen Proving Ground, MD, April 2010.

Appendix. The Catenary Solution

The catenary is a textbook problem in the teaching of differential equations. Historically, it refers to the shape a chain (or cable) assumes under the influence of gravity, being attached only at its endpoints. We rederive the result here for the convenience of the reader.

The governing equation to solve is functionally identical to that given in equation 5, namely:

$$u'' - a\sqrt{1 + u'^2} = 0 \quad . \quad (\text{A-1})$$

We reduce the equation order by casting u'' as $du'/du \cdot du/dx$, knowing that du/dx is the same as u' . In so doing, we obtain

$$\frac{u' du'}{\sqrt{1 + u'^2}} = a du \quad . \quad (\text{A-2})$$

This is readily integrated as

$$\sqrt{1 + u'^2} = au + C_1 \quad . \quad (\text{A-3})$$

Now we note that, in equation A-1, a vertical shift of magnitude u_{shift} , such that $\bar{u} = u - u_{\text{shift}}$ produces the identical equation in \bar{u} . This indicates that any solution, $u(x)$ is likewise a solution $\bar{u}(x)$. The vertical shift is related to constant C_1 . Therefore, we may choose any particular value of C_1 , for mathematical convenience, knowing that any solution subsequently obtained for $u(x)$ can be subjected to an arbitrary vertical shift. We choose C_1 so that u' is identically zero, when u is zero. Such a choice forces C_1 to a value of 1. With this substitution, equation A-3 becomes

$$\frac{du}{\sqrt{u}\sqrt{u + 2/a}} = a dx \quad . \quad (\text{A-4})$$

Introducing the substitution $v^2 = u$ reduces the subsequent integral of equation A-4 to a convenient form:

$$\int \frac{dv}{\sqrt{v^2 + 2/a}} = \int \frac{a}{2} dx \quad . \quad (\text{A-5})$$

The left-side integral may be solved in the following way:

$$\begin{aligned} \int \frac{dx}{\sqrt{x^2 + b}} &= \int \frac{(x + \sqrt{x^2 + b^2})dx}{(x + \sqrt{x^2 + b^2})\sqrt{x^2 + b}} = \int \frac{\left(1 + \frac{x}{\sqrt{x^2 + b^2}}\right) dx}{x + \sqrt{x^2 + b^2}} \\ &= \ln(x + \sqrt{x^2 + b^2}) + C \end{aligned} \quad (\text{A-6})$$

With this integration form, equation A-5 may be integrated as

$$\ln(v + \sqrt{v^2 + 2/a}) = (a/2)x + \ln C_2 \quad . \quad (\text{A-7})$$

Equation A-7 may be explicitly solved for v to yield

$$v = \frac{C_2}{2} e^{ax/2} - \frac{1}{aC_2} e^{-ax/2} \quad . \quad (\text{A-8})$$

Squaring this equation and substituting u for v^2 gives the following:

$$u = \frac{C_2^2}{4} e^{ax} + \frac{1}{a^2 C_2^2} e^{-ax} - 1/a \quad . \quad (\text{A-9})$$

Equation A-9 is equivalent to the form

$$u = Ae^{-ax} + Be^{ax} + C \quad , \quad (\text{A-10})$$

where A and B are subject to the constraint $2\sqrt{AB} = 1/a$. We see that the solution, given by equation A-10, matches the form presented in the report as equation 6, subject to the identical constraint on A and B . Often, in the literature, the result is given in terms of the equivalent hyperbolic cosine function.

For the general catenary solution (which may be shifted vertically), C is a free constant. If the constraint is enforced to make $u' = 0$ when $u = 0$ (as was enforced when we chose C_1), then C will take on a value of $-1/a$, as dictated by equation A-9. This constrained value of C was indeed obtained in the report as equation 14, in which C was revealed as $-1/\alpha$.

NO. OF
COPIES ORGANIZATION

1 DEFENSE TECHNICAL
(PDF INFORMATION CTR
ONLY) DTIC OCA
8725 JOHN J KINGMAN RD
STE 0944
FORT BELVOIR VA 22060-6218

1 DIRECTOR
US ARMY RESEARCH LAB
IMNE ALC HRR
2800 POWDER MILL RD
ADELPHI MD 20783-1197

1 DIRECTOR
US ARMY RESEARCH LAB
RDRL CIM P
2800 POWDER MILL RD
ADELPHI MD 20783-1197

1 DIRECTOR
US ARMY RESEARCH LAB
RDRL CIM L
2800 POWDER MILL RD
ADELPHI MD 20783-1197

ABERDEEN PROVING GROUND

1 DIR USARL
RDRL CIM G (BLDG 4600)

NO. OF
COPIES ORGANIZATION

3 DE TECHNOLOGIES INC
R CICCARELLI
W CLARK
W FLIS
3620 HORIZON DRIVE
KING OF PRUSSIA PA 19406

ABERDEEN PROVING GROUND

80 DIR USARL
RDRL SL
J BEILFUSS
R COATES
RDRL SLB
R BOWEN
G KUCINSKI
RDRL SLB A
D FARENWALD
L A BOMBOY
G BRADLEY
R DIBELKA
P HORTON
E HUNT
D PLEFKA
J ROBERTSON
RDRL SLB D
R GROTE
L MOSS
J POLESNE
RDRL SLB E
M MAHAFFEY
A M DIETRICH
R SAUCIER
RDRL SLB G
P MERGLER
J ABELL
C STANCOFF
RDRL SLB S
S SNEAD
R BOWERS
M OMALLEY
RDRL SLB W
L ROACH
RDRL WML D
A ZIELINSKI

NO. OF
COPIES ORGANIZATION

RDRL-WML-H
C CANDLAND
T EHLERS
T FARRAND
M FERREN-COKER
E KENNEDY
L MAGNESS
C MEYER
D SCHEFFLER
S SCHRAML
B SORENSEN
R SUMMERS
RDRL WMM B
G GAZONAS
RDRL WMP
S SCHOENFELD
RDRL-WMP-A
J POWELL
RDRL-WMP-B
C HOPPEL
S R BILYK
D CASEM
J CLAYTON
D DANDEKAR
M GREENFIELD
Y I HUANG
B LEAVY
B LOVE
M RAFTENBERG
M SCHEIDLER
T WEERISOORIYA
C WILLIAMS
RDRL-WMP-C
T W BJERKE
J BARB
N BRUCHEY
R MUDD
S SEGLETES
W WALTERS
RDRL-WMP-D
J RUNYEON
R FREY
V HERNANDEZ
S HUG
M KEELE
D KLEPONIS
H W MEYER
B SCOTT
K STOFFEL

NO. OF
COPIES ORGANIZATION

RDRL-WMP-E
M BURKINS
S BARTUS
W A GOOCH
E HORWATH
C KRAUTHAUSER
M LOVE
RDRL-WMP-F
N GNIAZDOWSKI
R BITTING
RDRL-WMP-G
D KOOKER
B KRZEWINSKI
S KUKUCK
J STARKENBERG

INTENTIONALLY LEFT BLANK.